

THE TURBULENT WALL-JET WITH HEAT TRANSFER

by

Aaron Christopher Jones

A Thesis Submitted to the Faculty of the

DEPARTMENT OF AEROSPACE AND MECHANICAL ENGINEERING

In Partial Fulfillment of the Requirements
For the Degree of

MASTER OF SCIENCE
WITH A MAJOR IN MECHANICAL ENGINEERING

In the Graduate College

THE UNIVERSITY OF ARIZONA

1996

STATEMENT BY AUTHOR

This thesis has been submitted in partial fulfillment of requirements for an advanced degree at the University of Arizona and is deposited in the University Library to be made available to borrowers under rules of the Library.

Brief quotations from this thesis are allowable without special permission, provided that accurate acknowledgment of source is made. Requests for permission for extended quotation from or reproduction of this manuscript in whole or in part may be granted by the head of the major department or the Dean of the Graduate College when in his or her judgment the proposed use of the material is in the interests of scholarship. In all other instances, however, permission must be obtained from the author.

SIGNED: _____

APPROVAL BY THESIS DIRECTOR

This thesis has been approved on the date shown below:

Israel J. Wagnanski
Professor of Aerospace and Mechanical Engineering

Date

ACKNOWLEDGMENTS

Throughout the course of this research, a number of individuals have provided useful assistance. I would especially like to thank Dr. Ming de Zhou for taking the time to answer my numerous questions and for providing the necessary impetus to complete the work, as well as Dr. Michael Amitay for his assistance in many aspects of the research. I also appreciate the assistance of Oleg Likhachev, Morris Kaufman, Ralf Neuendorf, and Kevin Elsberry. Finally, I would like to thank Dr. Israel Wygnanski for giving me the opportunity to work with his outstanding group of researchers and Drs. Hermann Fasel and Alfonso Ortega for reviewing this thesis.

This work was supported by a grant from the Air Force Office of Scientific Research (grant number F49620-94-1-0131) and was monitored by Dr. James McMichael. Additional graduate student funding was provided by the University of Arizona in the form of a Graduate Fellowship.

TABLE OF CONTENTS

NOMENCLATURE	5
LIST OF FIGURES	6
ABSTRACT.....	7
1. INTRODUCTION	9
1.1. BACKGROUND	9
1.2. OBJECTIVES	13
2. THEORETICAL ASPECTS.....	15
2.1. REYNOLDS ANALOGY.....	15
2.2. BUOYANCY	16
3. EXPERIMENTAL ASPECTS.....	18
3.1. FACILITY	18
3.2. VELOCITY AND TEMPERATURE MEASUREMENT	19
3.3. PROBE CALIBRATION.....	20
3.4. THERMAL BOUNDARY CONDITIONS	23
3.5. DATA ACQUISITION.....	24
4. RESULTS	26
4.1. EFFECTS OF HEATING.....	26
4.2. EFFECTS OF SELECTIVE FORCING	41
4.3. REPEATABILITY	48
5. CONCLUSIONS AND RECOMMENDATIONS.....	52
REFERENCES	54

NOMENCLATURE

α	molecular thermal diffusivity
β	nondimensional frequency
b	jet exit height
δ_v	hydrodynamic wall-jet thickness; Y -location of $U_{m/2}$
δ_t	thermal wall-jet thickness
ε_M	eddy momentum diffusivity
ε_H	eddy thermal diffusivity
f	dimensional frequency
η	film-cooling effectiveness; $\eta = (T_{aw} - T_{inf}) / (T_j - T_{inf})$
J	jet exit momentum; $J = U_j^2 b$
ν	molecular momentum diffusivity; kinematic viscosity
Pr_t	turbulent Prandtl number
q_t''	turbulent heat flux
ρ	fluid density
θ	nondimensional temperature; $\theta = (T_w - T) / (T_w - T_{inf})$
R	velocity ratio; $R = (U_j - U_{inf}) / (U_j + U_{inf})$
τ_t	turbulent shear stress
T	mean temperature
T_{aw}	adiabatic wall temperature
T_{inf}	mean external stream temperature
T_j	mean jet exit temperature
$\langle t' \rangle$	root mean square temperature
T_w	mean wall temperature
U	mean velocity
U_{inf}	mean external stream velocity
U_j	mean jet exit velocity
$\langle u_j' \rangle$	root mean square jet exit velocity
U_m	local maximum mean velocity of the wall-jet
$U_{m/2}$	local half-maximum mean velocity in the outer region of the wall-jet
$\langle u' \rangle$	root mean square velocity
ξ	nondimensional streamwise distance from jet exit; $\xi = X J / \nu^2$
X	dimensional streamwise distance from jet exit
Y	normal distance from the wall
Y_m	normal distance from the wall to the location of maximum mean velocity

LIST OF FIGURES

FIGURE 1.1: Representative mean velocity profile of the strong wall-jet.	10
FIGURE 3.1: Wall-jet apparatus.	19
FIGURE 3.2: Hot- and cold-wire calibration apparatus.....	21
FIGURE 3.3: Temperature-dependent voltage variation of the hot-wire at various velocities.	22
FIGURE 4.1: The dependence of velocity and length scales on $\xi = X J / v^2$ in the unheated, turbulent wall-jet.....	27
FIGURE 4.2: Mean velocity profile for the unheated reference case at several streamwise locations.	28
FIGURE 4.3: Fluctuating velocity profile for the unheated reference case at several streamwise locations.	29
FIGURE 4.4: Streamwise collapse of nondimensional mean velocity for the unheated reference case; lack of self-similarity in near-wall region.	30
FIGURE 4.5: Streamwise decay of maximum mean velocity with and without heating.....	32
FIGURE 4.6: A comparison of local length scales with and without heating.....	33
FIGURE 4.7: Mean temperature profile at various streamwise locations with the heated plate.	35
FIGURE 4.8: Fluctuating temperature profile at various streamwise locations with the heated plate.....	36
FIGURE 4.9: Streamwise collapse of nondimensional mean temperature with the heated plate; lack of self-similarity in near-wall region.	37
FIGURE 4.10: Streamwise collapse of nondimensional fluctuating temperature with the heated plate when scaled by the maximum local temperature r.m.s.....	38
FIGURE 4.11: A comparison of unheated reference and heated mean velocity profiles at two streamwise locations.	39

FIGURE 4.12: A comparison of unheated reference and heated fluctuating velocity profiles at two streamwise locations.	40
FIGURE 4.13: Collapse of mean velocity profiles for unheated reference and heated cases at two streamwise locations; lack of self-similarity in near-wall region.	41
FIGURE 4.14: Unforced (a) and forced (b) waveforms ($X/b = 40$; inner $0.35U_m$).	43
FIGURE 4.15: Effect of forcing on shear stress and wall temperature; 48 Hz and 91 Hz at $\langle u_j' \rangle / U_j \sim 10\%$, with and without a wall heating.	45
FIGURE 4.16: Effect of forcing on shear stress and wall temperature; 48 Hz and 91 Hz at $\langle u_j' \rangle / U_j \sim 10\%$, with and without a wall heating (normalized by maximum reductions in shear stress and wall temperature).	47
FIGURE 4.17: Repeatability of mean velocity profiles for unheated reference case.	49
FIGURE 4.18: Repeatability of mean velocity profiles for heated wall case.	50
FIGURE 4.19: Repeatability of mean temperature for heated wall case.	51

ABSTRACT

The plane, turbulent wall-jet with heat transfer was investigated experimentally: one case with an adiabatic wall and another with a surface of arbitrary heat flux. Mean and fluctuating velocities and temperatures were mapped using hot- and cold-wire anemometry, respectively, and disturbances were introduced at specific frequencies in an effort to control wall temperature and skin friction. In the case of the heated wall, forcing was found to decrease both wall temperature and skin friction regardless of frequency, likely augmenting the interaction between vortical structures in the cool outer region of the jet with those in the hot inner region. Reductions in wall shear stress of as much as 22% were observed with a simultaneous reduction in the local temperature scale of 4%. These promising results suggest that periodic modulation of the turbulent wall-jet is a viable technique for reducing aerodynamic drag and increasing heat transfer.

1. INTRODUCTION

1.1. BACKGROUND

A *wall-jet* is a jet of fluid blown tangentially along a solid surface of arbitrary curvature. The jet can be embedded in the wall boundary layer of a co-flowing external stream or it can exist in the absence of an external flow. Wall-jets are generally classified as either *strong* or *weak*, depending on the ratio of the mean external stream velocity to the maximum mean jet velocity. If the velocity of the co-flowing external stream is less than half of the maximum jet velocity, then the wall-jet is said to be “strong”; otherwise, it is called “weak”. Both strong and weak wall-jets have important engineering applications that necessitate a thorough understanding of the flow.

Wall-jets are widely used for film-cooling, evaporation enhancement, and boundary layer control. They are applied to turbine blades and rocket nozzles, for example, in order to shield them from hot and/or corrosive flow environments. A wall-jet flow that is cooler than the external stream acts as a protective buffer for the surface, thus easing stringent material temperature requirements. Wall-jets are applied to windshields and windows as defrosters in order to enhance evaporation, and they are present with aircraft slotted flaps and leading edge slats, enabling increased lift and delayed flow separation. Given its many engineering applications, it is no wonder that there have been well over two hundred reports describing various applications of the turbulent wall-jet. In-depth surveys of past experimental investigations are provided by Launder and Rodi^{1,2}.

Zhou *et al.*³ concluded that the strong wall-jet can be thought of as a combination of two shear layers, as is apparent from the representative mean velocity profile shown in Figure 1.1. Its inner region resembles a conventional wall boundary layer while its outer region resembles a free shear layer.

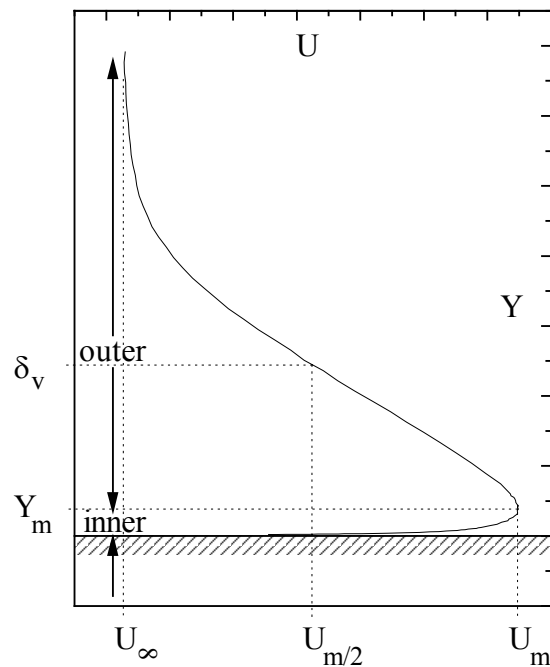


FIGURE 1.1: Representative mean velocity profile of the strong wall-jet.

The strong wall-jet accordingly has two modes of hydrodynamic instability: a viscous mode associated with the velocity gradient in the inner region and an inviscid mode associated with the inflection point in the outer region. Large vortices resulting from the inviscid instability exist in the outer region. In the turbulent wall-jet, the interaction of these vortices with smaller ones in the inner region is not well understood, but recent investigations (e.g., Katz *et al.*⁴) have alluded to the possibility of controlling

hydrodynamic parameters such as skin friction by indirectly affecting these structures. This control is accomplished by *selective forcing* of the instability modes. “Selective forcing” means that artificial disturbances are introduced to the flow via periodic modulation at specific frequencies that are associated with the instability modes. Results have indicated that selective forcing can yield significant reductions in skin friction, but the effects of selective forcing on heat transfer are generally unknown.

Previous work on heat transfer in a pulsating, turbulent wall-jet or a pulsating jet injected into an external stream is apparently non-existent. The work of Lebedev *et al.*⁵, however, provides some useful insight. They observed that film-cooling effectiveness tends to decrease with increasing freestream turbulence, where the effectiveness is historically defined as

$$\eta = (T_{aw} - T_{inf}) / (T_j - T_{inf})$$

If flow turbulence can be thought of as a sort of natural forcing with a broad spectrum of frequencies, then disturbances at specific frequencies associated with instability modes in the flow should become most amplified. It may be that increasing freestream turbulence strengthens the dominance of the outer coherent structures over the small vortices in the inner region, thus augmenting transport normal to the wall and resulting in a decrease of the local temperature scale.

Additional insight can be obtained from a similar investigation by Moffat and Maciejewski⁶. They researched the role of the freestream turbulence level on heat

transfer to a flat plate in an axisymmetric jet and observed a 350% increase in the fully turbulent flat plate heat transfer. There are in fact many publications (including MacMullin *et al.*⁷) that demonstrate heat transfer augmentation in the presence of increased turbulence, for wall-jets as well as other flow geometries. Most of these investigations have been motivated by film-cooling applications and have specifically been directed at determining adiabatic wall temperature distributions under various conditions.

An excellent survey of early film-cooling investigations is provided by Goldstein⁸. Goldstein also discusses conventional heat transfer theory associated with film-cooling. He points out that the film-cooling geometry can be divided into three zones: Zone I for the film-cooled surface, Zone II in the region of the film-cooling hole, and Zone III in the internal cooling duct. The film-cooling heat transfer problem is a conjugate one and as such all three zones must be considered simultaneously when attempting to predict film-cooling effectiveness. The heat transfer is strongly dependent on the blowing ratio, the ratio of the injection velocity to the freestream velocity. As this ratio increases, the effect of freestream turbulence decreases. This was confirmed by Lebedev *et al.* and is likely due to the fact that the adiabatic wall temperature, and thus the film-cooling effectiveness, is a measure of the thermal mixing between the jet and the external flow. At low blowing ratios, turbulent eddies in the external flow can more readily transport thermal energy toward the wall, causing an increase in the wall temperature, than at higher blowing ratios.

The results of Dec and Keller⁹ and Arpaci *et al.*¹⁰ support the findings of Lebedev *et al.* as well as those presented by Goldstein. In an experimental investigation of the pulse combustor, Dec and Keller found that heat transfer from the hot flow to the wall of the combustor increases with the addition of velocity pulsations. Likewise, Arpaci *et al.* developed a model that actually predicts enhancement of the heat transfer coefficient above its steady state value in a pulse combustor.

An ongoing investigation by Quintana *et al.*¹¹ has demonstrated effects of selective forcing on heat transfer in the *laminar* wall-jet. With a strong, laminar wall-jet over an isothermal surface, selective forcing was applied in order to observe its effects on shear stress and heat flux. Selective forcing was found to decrease the wall shear stress as much as 70% and increase the local heat flux up to 35%. They hypothesized that the decrease in shear stress is due to a dominance of the large, outer vortices. These vortices likely increase the local heat flux by increasing transport away from the wall. It is desirable to complement results obtained for the laminar wall-jet with data for the turbulent wall-jet since the turbulent jet is the most important in engineering applications.

1.2. OBJECTIVES

Although it has been extensively studied in the past, the turbulent wall-jet is still poorly understood and our understanding of its heat transfer characteristics is especially poor. This is unfortunate considering its important thermal applications. This investigation is therefore intended to improve our understanding of the turbulent wall-jet with heat transfer. Specifically, the goals are (1) to design, fabricate, and qualify a wall-

jet facility suitable for a turbulent heat transfer investigation, (2) to spatially map the hydrodynamic and thermal streamwise development of the turbulent wall-jet, and (3) to determine if it is possible to manipulate heat transfer in the flow with the use of selective forcing. The strong, turbulent wall-jet in air with a plane boundary of arbitrary heat flux is investigated as is the heated, turbulent wall-jet over an plane, adiabatic surface. Both quantitative and qualitative results should provide a foundation for future work with more extreme temperatures and turbulence levels, varied thermal and geometric boundary conditions, and the addition of an external stream.

2. THEORETICAL ASPECTS

2.1. REYNOLDS ANALOGY

In a turbulent flow, it has become the convention to define the eddy momentum and thermal diffusivities (ε_M and ε_H) analogous to their molecular counterparts in laminar flow (ν and α) such that

$$\tau_t / \rho = \varepsilon_M dU/dY \text{ and } q_t'' / (\rho c) = \varepsilon_H dT/dY$$

where τ_t / ρ and $q_t'' / (\rho c)$ are the apparent turbulent shear stress and apparent turbulent heat flux in the direction normal to the main flow. For wall-bounded turbulent flows, $\varepsilon_M \gg \nu$ and $\varepsilon_H \gg \alpha$ in the fully turbulent region and $\nu \gg \varepsilon_M$ and $\alpha \gg \varepsilon_H$ in the viscous sublayer near the bounding surface.

Since the same turbulent motions give rise to both the shear stress and the heat flux, it follows that there may be a simple relationship between the eddy momentum and thermal diffusivities. The *Reynolds analogy* states that the eddy momentum and thermal diffusivities are equal, thus implying a turbulent Prandtl number of unity since

$$\text{Pr}_t = \varepsilon_H / \varepsilon_M$$

This ignores, however, the differences in the momentum and thermal exchange mechanisms; i.e., momentum variables are vectors while thermodynamic ones are scalars. For classes of turbulent flows where time-averaging is adequate, the differential equations governing the flow can be reduced to ones similar to those for steady laminar

flows. In these cases the Reynolds analogy is found to be suitable. However, turbulent flows are inherently unsteady due to the presence of small-scale vorticity, and time-averaging can consequently cause problems due to the vectorial nature of the momentum variables (Kays and Crawford¹²).

From the Reynolds analogy, it is apparent that observations of shear stress reductions in the presence of selective forcing may be accompanied by changes in heat flux. It is unknown, however, what the effect on heat flux will be since the externally-excited turbulent wall-jet is highly unsteady. Indeed, Dec and Keller ascertained that the Reynolds analogy does not hold for their highly unsteady pulse combustor flow, stating the importance of the difference between the momentum and thermodynamic transfer mechanisms.

2.2. BUOYANCY

In the presence of large temperature differences between the wall or jet and the external stream, the effects of buoyancy may be non-negligible. In the case of the wall-jet, a high wall temperature relative to the jet temperature could cause the existence of an additional hydrodynamic instability mode and other significant alterations of the velocity field. Temperatures and velocities are chosen such that this is not allowed to happen. To predict the importance of buoyancy, the ratio of the buoyancy forces to inertial forces is estimated. The ratio of the Grashof number to the square of the Reynolds number is the figure of merit. If this ratio is $\ll 1$, then the effects of buoyancy are assumed to be negligible. Order of magnitude analysis indicates that it is on the order of 10^{-1} for this

investigation. Buoyancy, therefore, is not expected to affect the velocity field significantly.

3. EXPERIMENTAL ASPECTS

3.1. FACILITY

This investigation was conducted in the William Sears wind tunnel at the University of Arizona. The test section of this low-speed, open-return tunnel was outfitted with a three-axis, motorized traversing mechanism which enabled accurate positioning of hot- and cold-wire probes in the wall-jet for velocity and temperature measurement, respectively; the X and Y resolutions were both 0.00125 mm.

Flow entered the test section from the wall-jet apparatus and moved tangentially over a plane, thermally-controlled surface that comprised the test section floor. The wall-jet apparatus is composed of a diffuser followed by a series of three screens of decreasing mesh size and a contraction. The jet exits from an adjustable slot, adhering to a 2-in diameter cylinder, and flows over the thermally-controlled test surface. Selective forcing of the wall-jet is accomplished by sending a sinusoidal signal of known frequency and amplitude to a subwoofer which is attached to the diffuser, consequently causing pressure fluctuations of the jet. Temperature control of the jet is possible using an inline air-water heat exchanger upstream of the diffuser. A schematic of the wall-jet apparatus is shown in Figure 3.1.

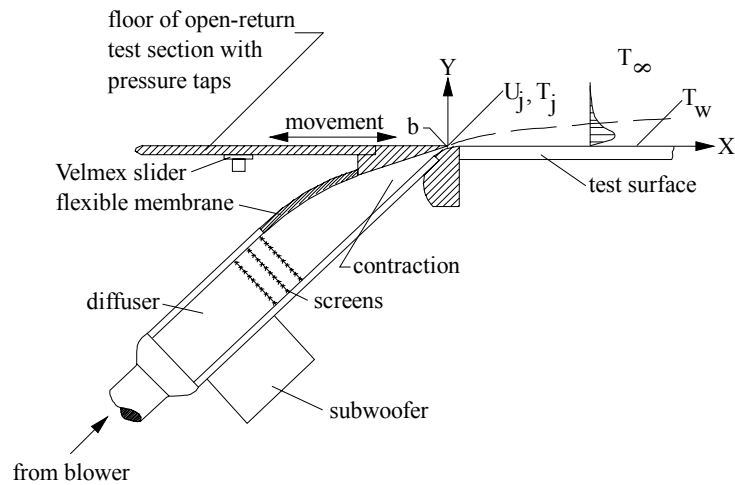


FIGURE 3.1: Wall-jet apparatus.

3.2. VELOCITY AND TEMPERATURE MEASUREMENT

Mean and fluctuating velocities and temperatures were measured using hot- and cold-wire anemometry, respectively. Dantec P-11 probes with 5- μm tungsten wire allowed adequate spatial resolution and frequency response using an A.A. Lab Systems AN-1003 anemometer with constant-temperature and constant-current bridges. The probes were mounted in a small, aerodynamic fixture separated by a center-to-center distance of 4.5 mm in the spanwise direction. Variations of the velocity and temperature profiles were observed to be negligible over the distance between two wires for each of the cases under investigation.

Great care was taken to ensure that the wires were as parallel to the measurement surface as possible; previous measurements indicated a noticeable sensitivity of the near-wall velocity and temperature data to slight rotations. Alignment was accomplished using a small telescope and a plane mirror. The telescope enabled an enlarged view of

the probes, while the plane mirror was used at a 45° angle to provide a view of the probes from the streamwise direction. The probes were leveled with respect to the surface and with respect to each other.

3.3. PROBE CALIBRATION

A special calibration apparatus was fabricated specifically for the probes used in this investigation. The apparatus consists of two inline air-water heat exchangers upstream of honeycomb, screen, and a 20:1 nozzle. A thermally insulated enclosure is used to help ensure uniformity of the jet exit temperature distribution and to optimize the maximum and minimum temperatures that can be achieved. In order to remove variations in the jet exit temperature profile caused by buoyancy, the apparatus was designed to be vertical. This resulted in uniform jet exit temperature and velocity profiles. The probes were calibrated at the jet exit by mounting them at a 10° angle to the flow, the angle used in subsequent measurements. A motorized angular positioning mechanism was added to enable the calibration of x-wire probes. Figure 3.2 shows a schematic of the calibration apparatus.

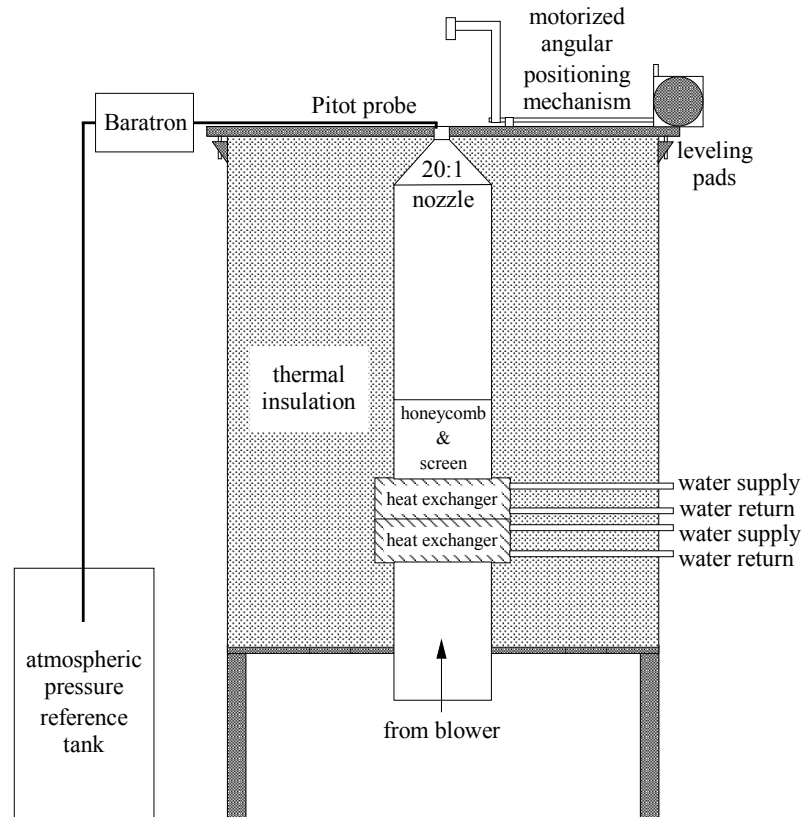


FIGURE 3.2: Hot- and cold-wire calibration apparatus.

Calibration of the cold-wire was performed at the thermally controlled jet exit against a K-type (chromel-alumel) thermocouple. The voltage output of the constant-current bridge was found to be linearly dependent on temperature, namely $T (^{\circ}\text{C}) = 1.665 \text{ V (Volts)} + 31.536$. After this calibration, the cold-wire was used to temperature-compensate the hot-wire.

The voltage output of the constant-temperature bridge varies as a function of both flow velocity and temperature. It is necessary, therefore, to adjust the voltage for temperature changes in order to obtain an accurate measurement of velocity. In the case

of the variation with temperature, the voltage output varies linearly. As the velocity decreases, however, the rate of change of the voltage with respect to temperature decreases as illustrated in Figure 3.3.

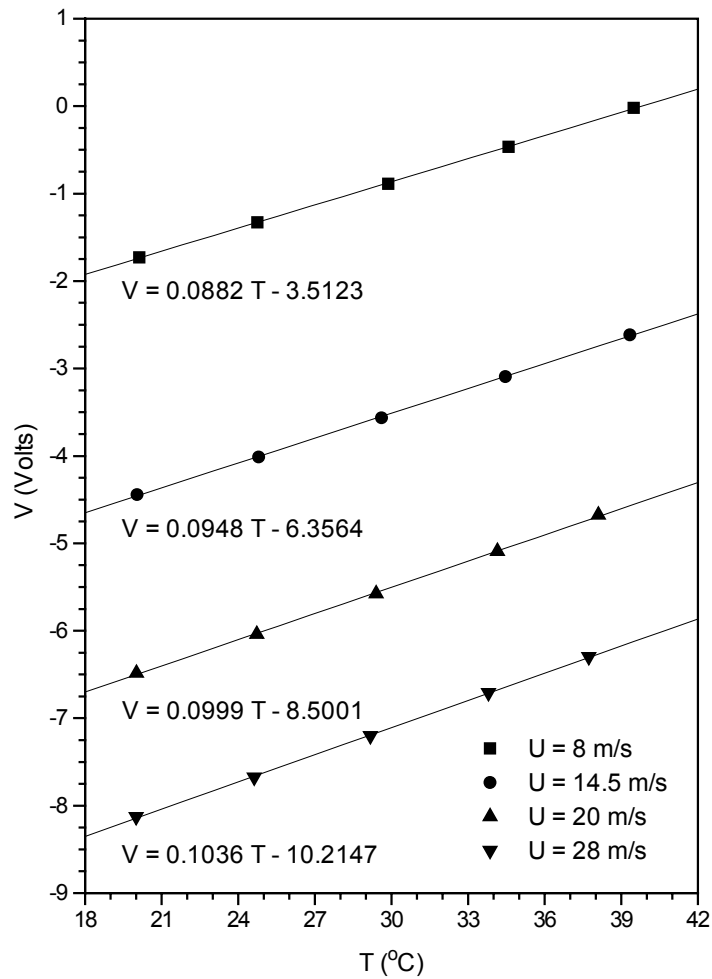


FIGURE 3.3: Temperature-dependent voltage variation of the hot-wire at various velocities.

Instead of utilizing a variable slope for subsequent measurements, a constant slope of $0.098 \text{ V}/^\circ\text{C}$ was assumed. Although this causes error in the measurement, it greatly

simplifies the data collection procedure and was necessary given the time constraints of this research.

The hot-wire was then calibrated at twelve different velocities (against a 10-Torr Baratron pressure transducer) for a constant temperature and the data was fit with a fourth order polynomial. The velocities ranged from 0 m/s to 28 m/s in order to cover the large distribution of velocities in the turbulent wall-jet. With this calibration in hand, it is possible to measure velocity and temperature simultaneously in the flow. Knowing the variation of the hot-wire voltage with temperature as well as the calibration temperature of the wire, the hot-wire signal can be corrected and, thus, the effects of velocity and temperature on the signal can be separated.

3.4. THERMAL BOUNDARY CONDITIONS

Two thermal boundary conditions were developed for this investigation, one adiabatic surface and one surface of arbitrary heat flux. Both surfaces measure 2 ft in the spanwise direction and 3 ft streamwise. The adiabatic surface consists of three layers bonded with spray adhesive: a lower 5/8-in thick high-density particle board substrate for rigidity, a 1-in thick piece of Dow Styrofoam for insulation, and an upper 0.005-in thick piece of fiberglass for flow-side surface quality. Particle board provides rigidity and a good bonding surface for the insulation, while rigid, extruded polystyrene foam was chosen because of its low thermal conductivity, its isotropy, and its availability. Although the thermal conductivity of the fiberglass sheet is high, its effect on the system is assumed to be negligible due to its minute thickness relative to the other layers. The

thermal time constant of the surface also played an important role in the material selection process. Relative differences between various material candidates were evaluated with the goal of minimizing the time constant.

Because changes in adiabatic wall temperature were not resolvable using the maximum achievable jet exit temperature, the adiabatic surface was not used for the majority of this investigation. Instead, a prototype surface of arbitrary heat flux was developed that enabled the attainment of much higher temperatures. The purpose of this surface was to determine whether or not surface temperature can be affected with the application of selective forcing. The arbitrary heat flux surface was comprised of a 0.5-in thick piece of aluminum atop four flat rubber resistance heaters placed adjacent to one another in the streamwise direction. The heaters were individually powered by a 4-channel ac power supply and were held in place by a 0.25-in thick piece of aluminum from below. The surface heat flux was found to be initially constant when disturbances were introduced to the flow although changes in surface temperature were observed. Both surface temperature and heat flux, however, changed over long periods of time.

3.5. DATA ACQUISITION

Data was acquired using a 486/66 personal computer with a LabVIEW interface. A National Instruments AT-MIO-16E-2 A/D board and an AT-AO-6 D/A board were utilized. The 12-bit A/D board provided a resolution of 0.0048 V, resolving temperature changes from the cold-wire signal as low as 0.008 °C. All mean data was collected using a sampling frequency of 600 Hz, being limited by frequency response of the cold-wire.

Each analog sample was digitized into 512 points and a total of 150 digitized analog samples were averaged at each measurement station. These parameters were chosen such that the measurement time for one profile was minimized without compromising repeatability due to thermal variations in the environment. All data was subsequently stored on magnetic tape.

4. RESULTS

Four cases were investigated with the surface of arbitrary heat flux, each using a jet exit Reynolds number of approximately 5,760 ($U_j = 27$ m/s and $b = 3.2$ mm). This Reynolds number, although somewhat arbitrary, was chosen for three reasons: (1) the desire to have a jet which was turbulent at the exit, (2) the need to introduce disturbances to the flow at an order of $\langle u_j' \rangle / U_j \sim 10\%$ with the power limitations of an existing amplifier and speaker, and (3) the need to avoid rotational frequencies of the wall-jet blower that yield undesirable jet disturbances at specific frequencies. The first case under investigation was an unheated reference case without selective forcing. This was followed by the addition of heating, then the addition of forcing both with and without heating. The adiabatic surface was generally not used as mentioned in section 3.4.

4.1. EFFECTS OF HEATING

The unheated reference case was found to agree well with previous turbulent wall-jet investigations. This case was primarily used to qualify the facility and measurement technique to the extent that the present data agreed with historical data. As shown in Figure 4.1, the streamwise variations of the maximum mean velocity, the Y-location of the maximum mean velocity, and the wall-jet thickness each obey power laws in fair agreement with those stated by Wygnanski, *et al.*¹³. In fact, Wygnanski *et al.* determined that the bulk of the flow is self-similar provided it is scaled by the momentum flux at the jet exit and by the kinematic viscosity of the fluid. These correlations may be

used to predict the behavior of incompressible wall-jets provided the maximum mean velocity of the jet is at least twice as large as the local external stream velocity.

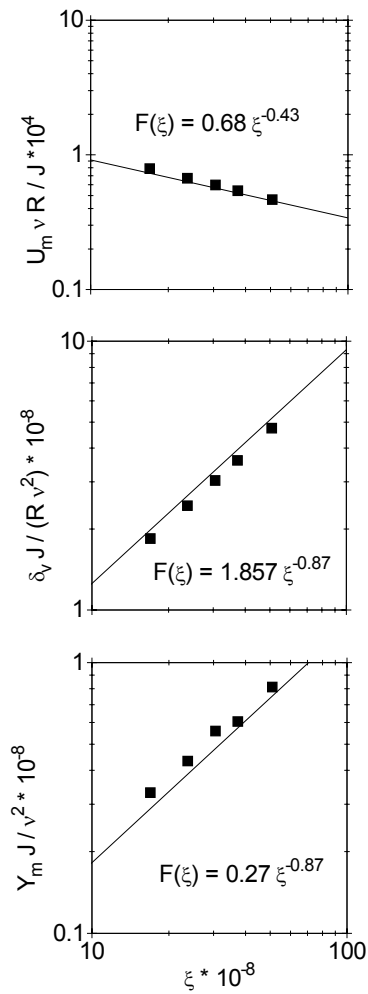


FIGURE 4.1: The dependence of velocity and length scales on $\xi = X J / v^2$ in the unheated, turbulent wall-jet.

Additionally, the streamwise development of the mean and fluctuating velocity profiles was found to be uneventful. Mean and fluctuating velocity profiles are shown in Figure 4.2 and Figure 4.3, respectively. As first observed by Glauert¹⁴, the turbulent

wall-jet is not self-similar. Figure 4.4 indicates, however, that the nondimensional mean velocity profiles collapse except in the near-wall region when the wall-jet thickness is chosen as the length scale and the local maximum mean velocity is taken as the velocity scale.

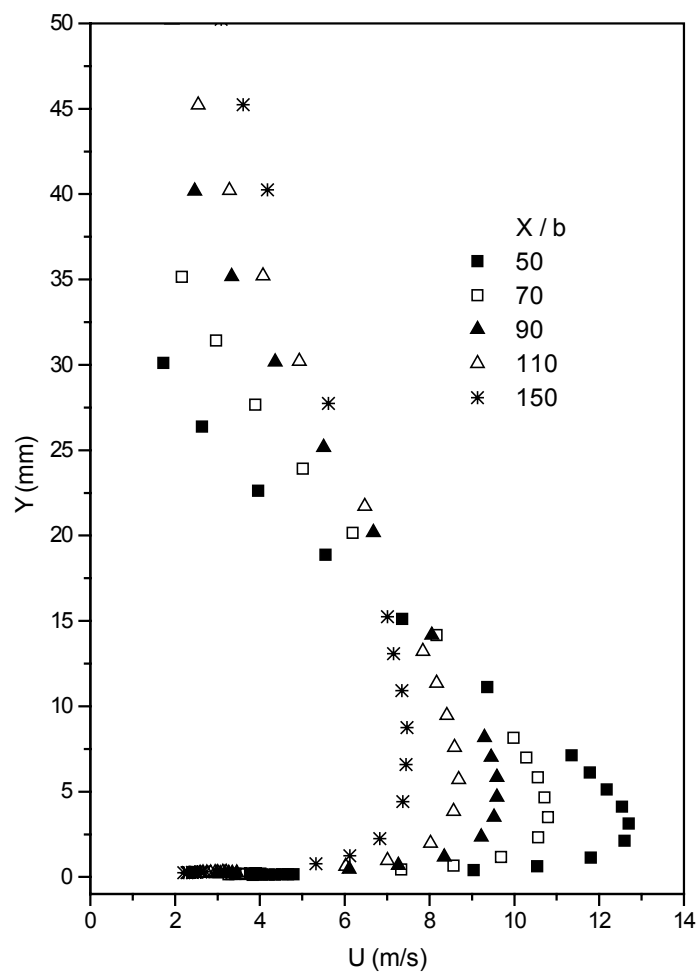


FIGURE 4.2: Mean velocity profile for the unheated reference case at several streamwise locations.

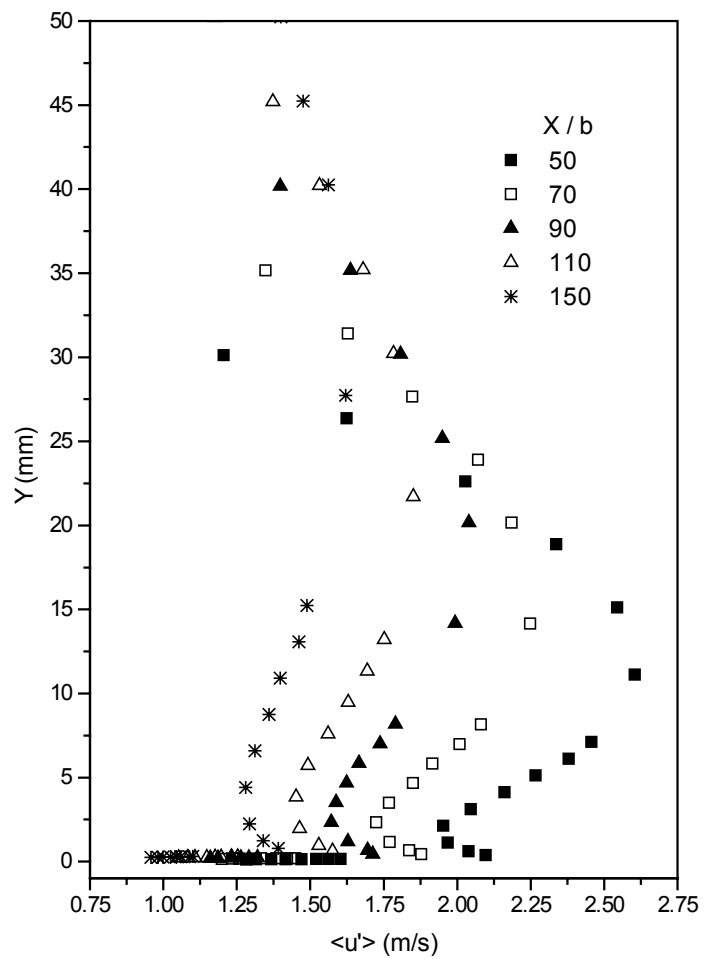


FIGURE 4.3: Fluctuating velocity profile for the unheated reference case at several streamwise locations.

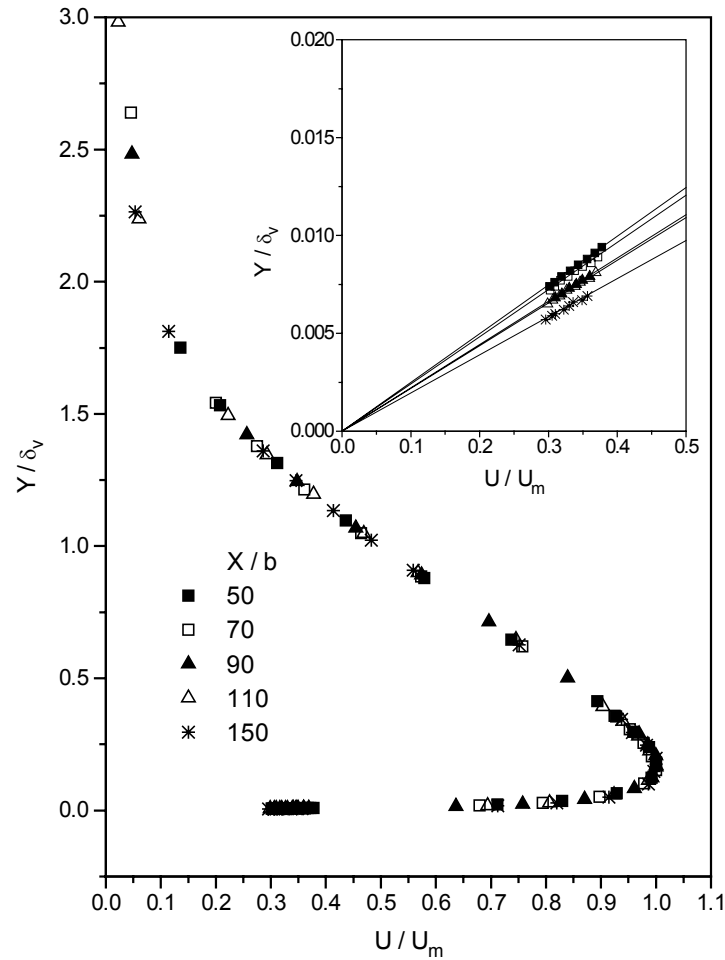


FIGURE 4.4: Streamwise collapse of nondimensional mean velocity for the unheated reference case; lack of self-similarity in near-wall region.

Like the unheated reference case, the heated wall case did not provide any surprises. In fact, the results confirm that buoyancy is not a problem with the selected temperatures and velocities. As shown in Figure 4.5, the streamwise decay of the maximum mean velocity compares favorably with the unheated reference case; the consistent difference in U_m is approximately 2% and is due to calibration error resulting

from the temperature compensation procedure (section 3.3). Wall-jet growth is compared in Figure 4.6 for the unheated reference and heated cases. Note that the heated plate causes negligible differences in the growth of δ_v and Y_m . Also note that the thickness of the thermal boundary layer, defined for convenience as the y -location where the temperature is equal to the average of the wall temperature and the freestream temperature, is small relative to the hydrodynamic thickness. For the case under investigation where the thermal boundary condition is ill-defined, δ_t is not particularly meaningful.

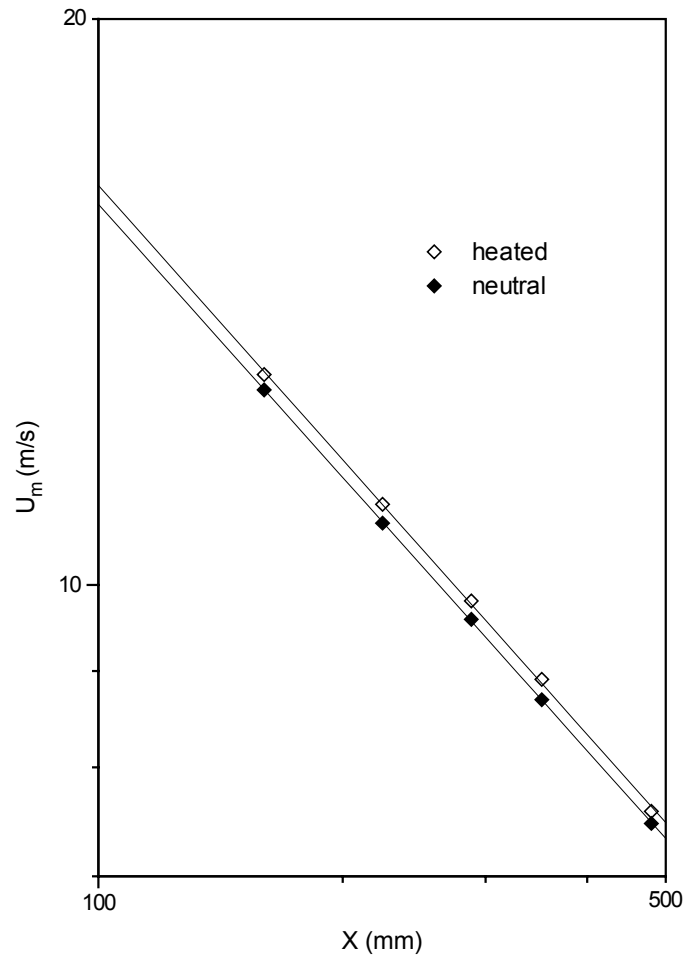


FIGURE 4.5: Streamwise decay of maximum mean velocity with and without heating.

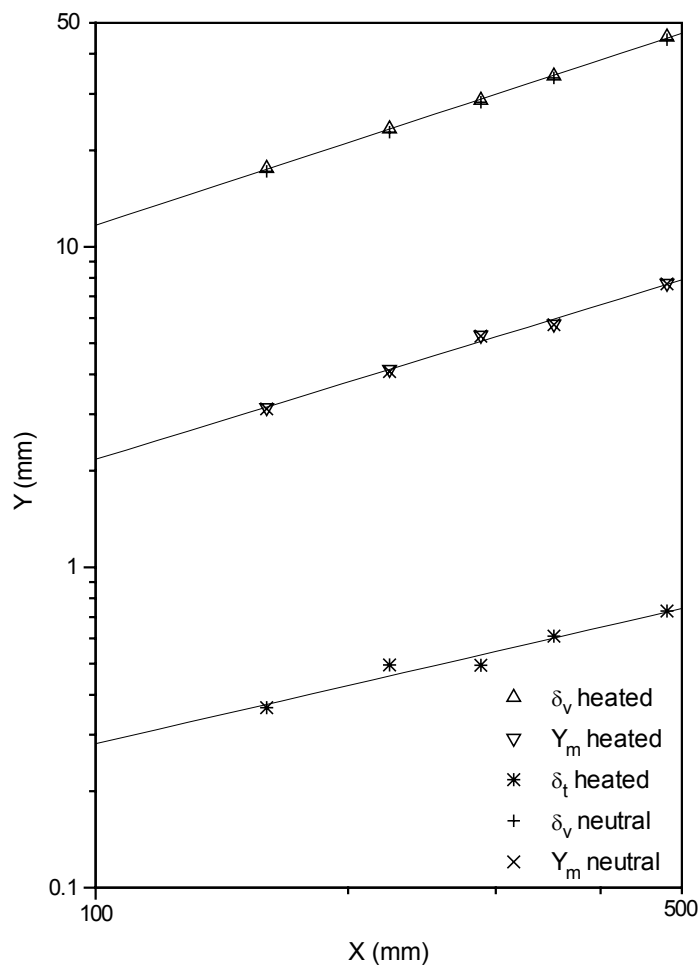


FIGURE 4.6: A comparison of local length scales with and without heating.

The streamwise development of the mean and fluctuating velocities is again normal, as is that of the mean and fluctuating temperatures which are shown in Figure 4.7 and Figure 4.8. As in the unheated reference case, collapse of the nondimensional mean velocity profiles is evident. A similar collapse (Figure 4.9) of the nondimensional mean temperature profiles is possible but is much more difficult to obtain since it is highly dependent on the establishment of a thermal steady state. Note that the temperature was

scaled by the difference between the wall temperature and the local freestream temperature despite the fact that a slight streamwise variation of the freestream temperature was observed even as high as 400 mm above the plate. The addition of an external stream might have eliminated the problem, but overheating of the wind tunnel motor prohibited its use. Like the nondimensional velocity profiles, the nondimensional temperature profiles exhibit a general streamwise increase in slope near the wall.

Collapse of the fluctuating temperature, shown in Figure 4.10, is apparent when it is nondimensionalized by the maximum local fluctuating temperature, suggesting that the same length scales affect both the mean temperature and the fluctuating temperature. A similar collapse of the fluctuating velocity profiles when scaled by the maximum fluctuating velocity is apparent in both the unheated reference and heated cases. Nondimensionalization by the previous temperature scale, namely $T_w - T_{inf}$, does not result in a collapse of the profiles because the temperature fluctuations are not in equilibrium with the mean. Likewise, lack of self-similarity is seen in the fluctuating velocity profiles with their failure to collapse when nondimensionalized by U_m (also observed by Wygnanski *et al.*). A streamwise increase of the nondimensional velocity and temperature fluctuations is observed in the inner region when scaled by these mean parameters.

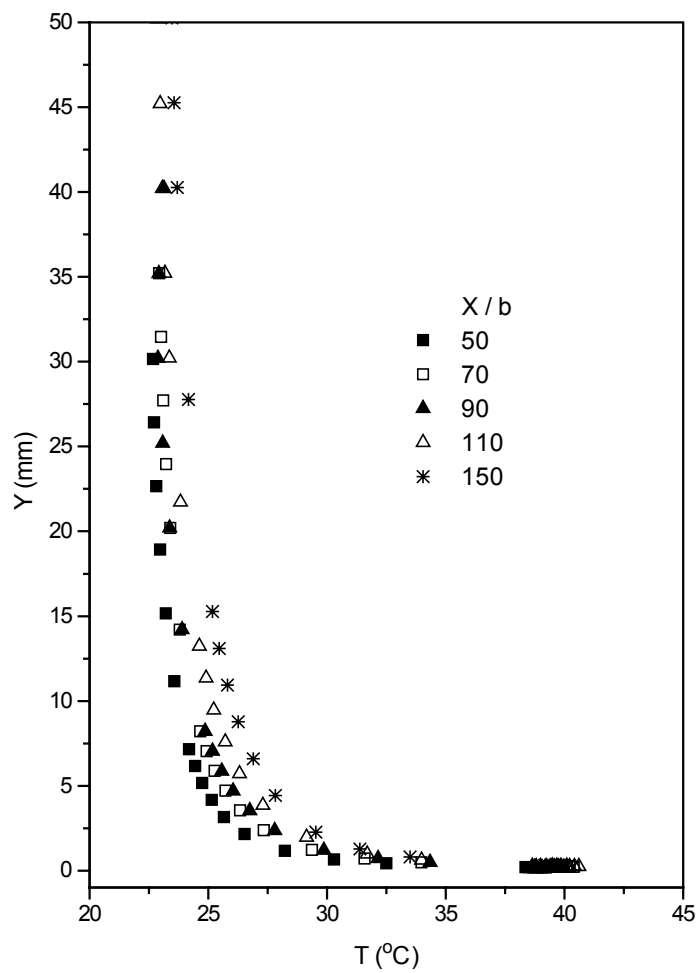


FIGURE 4.7: Mean temperature profile at various streamwise locations with the heated plate.

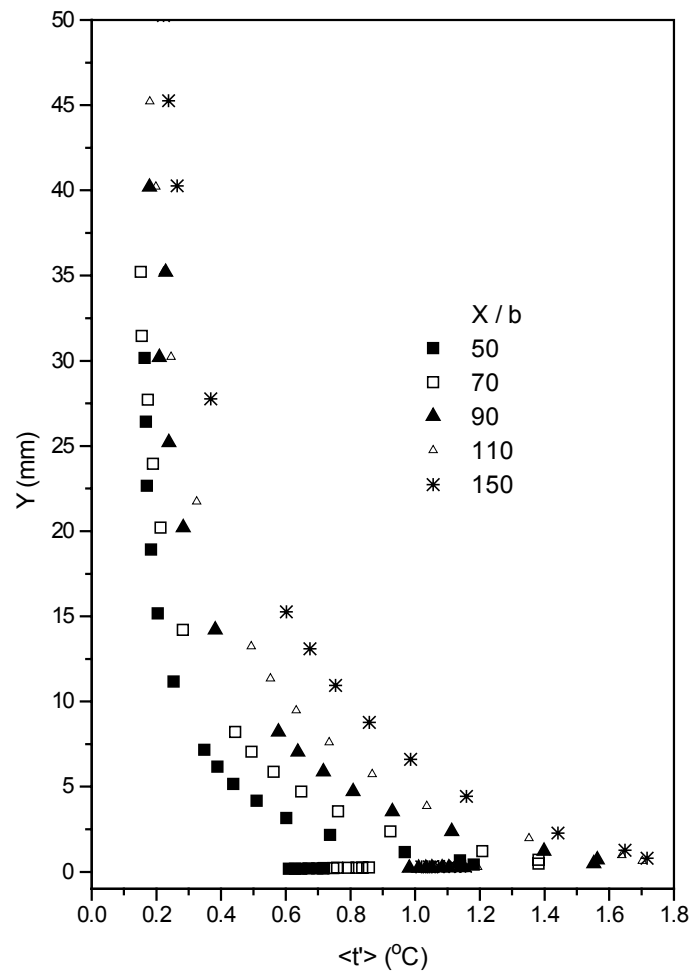


FIGURE 4.8: Fluctuating temperature profile at various streamwise locations with the heated plate.

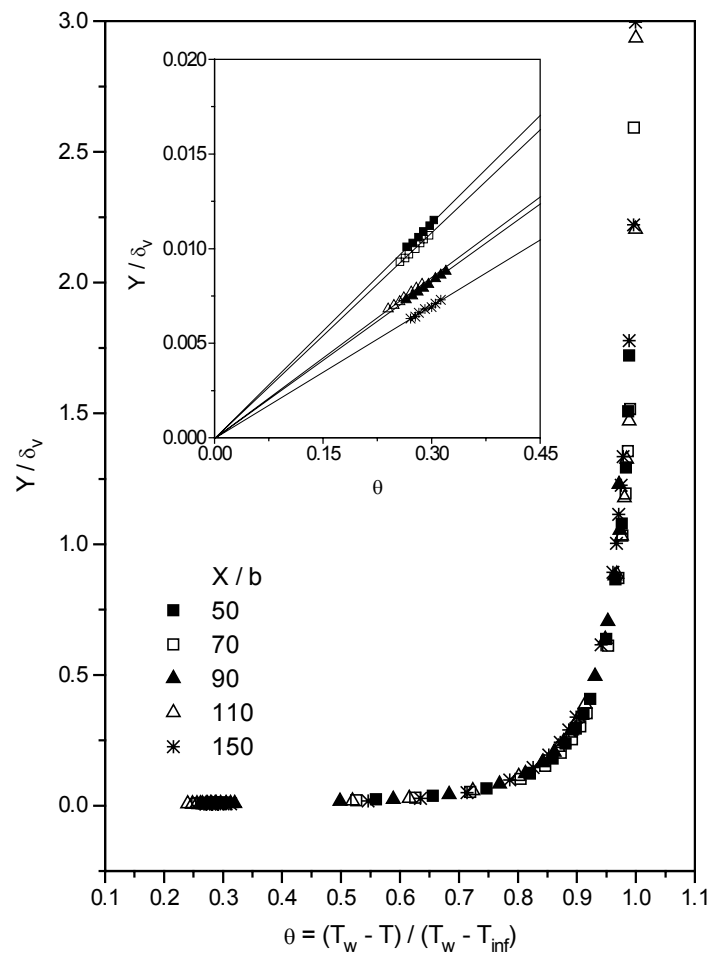


FIGURE 4.9: Streamwise collapse of nondimensional mean temperature with the heated plate; lack of self-similarity in near-wall region.

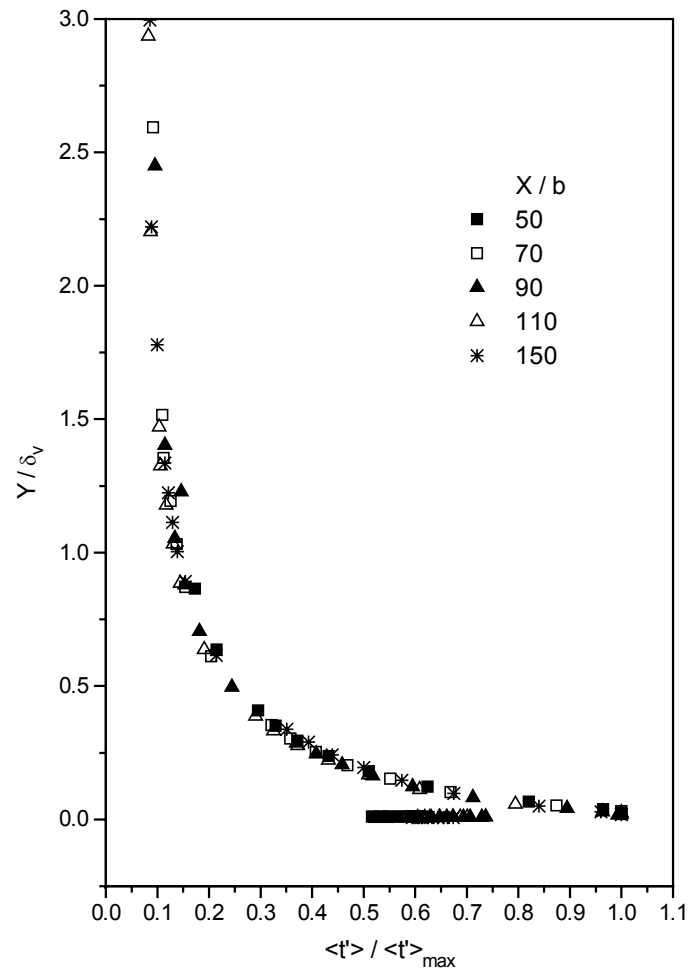


FIGURE 4.10: Streamwise collapse of nondimensional fluctuating temperature with the heated plate when scaled by the maximum local temperature r.m.s..

A comparison of the dimensional velocity profiles for the unheated reference and heated cases indicates that only minor changes in the profiles result from the application of heating. Heating causes an increase in molecular viscosity near the wall and an increase in fluctuations due to increased shear stress above the viscous sublayer. These changes are manifested in decreased wall shear stress (Figure 4.11) and increased r.m.s.

(Figure 4.12). Despite slight changes in the presence of heating, the nondimensional mean velocity profiles collapse with those of the unheated reference case as shown in Figure 4.13.

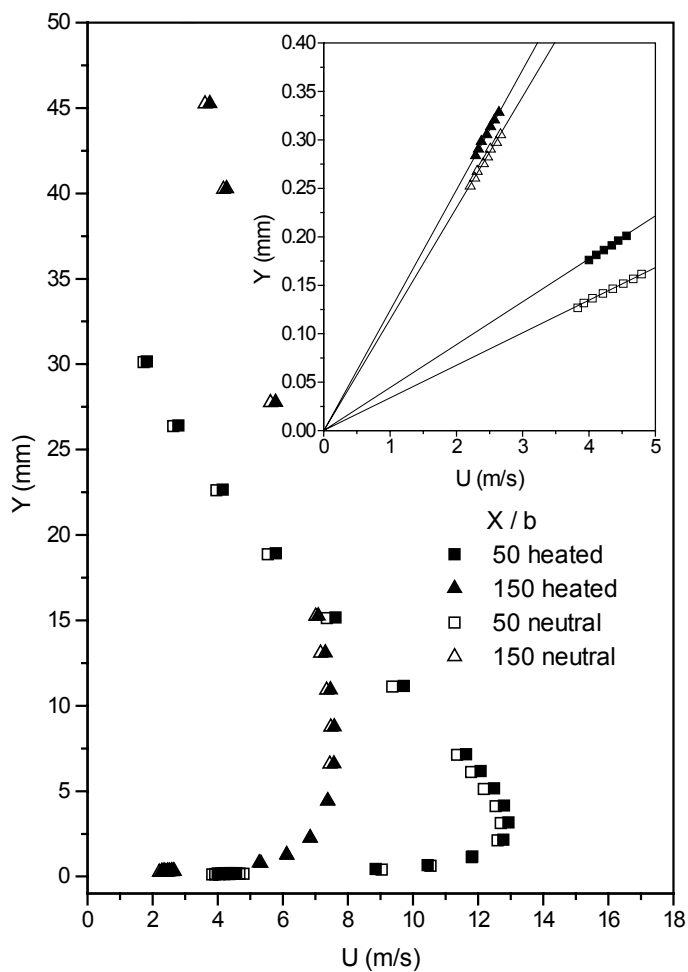


FIGURE 4.11: A comparison of unheated reference and heated mean velocity profiles at two streamwise locations.

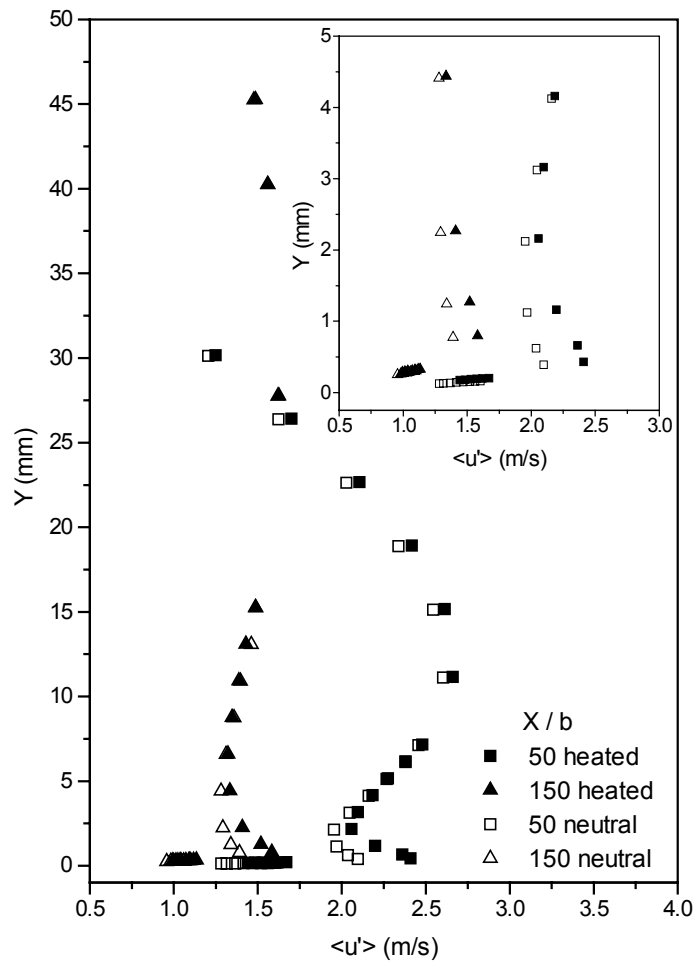


FIGURE 4.12: A comparison of unheated reference and heated fluctuating velocity profiles at two streamwise locations.

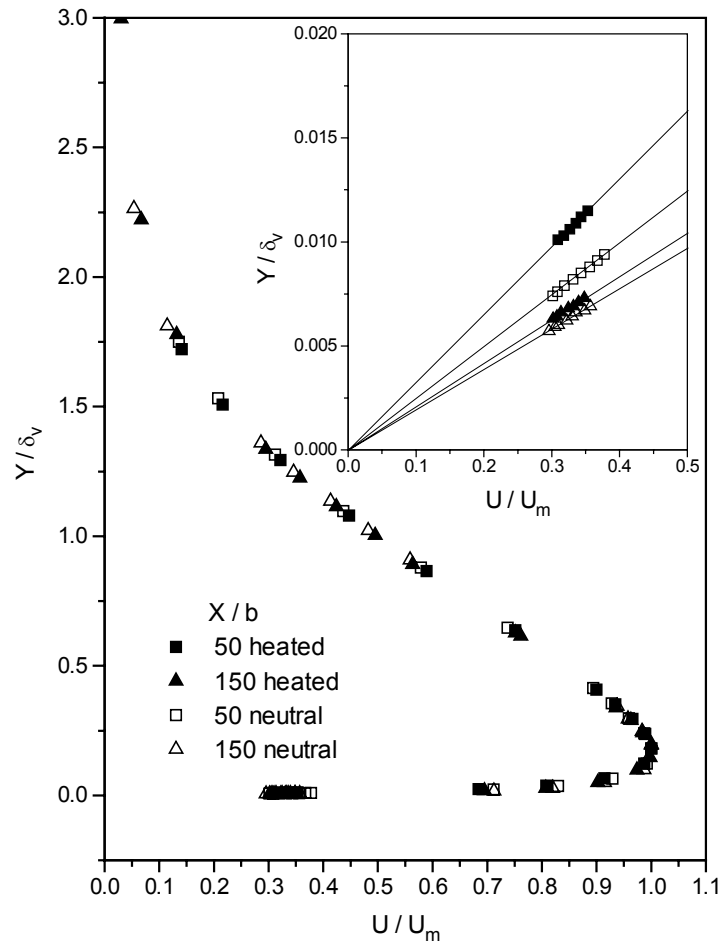


FIGURE 4.13: Collapse of mean velocity profiles for unheated reference and heated cases at two streamwise locations; lack of self-similarity in near-wall region.

4.2. EFFECTS OF SELECTIVE FORCING

The effects of selective forcing on the turbulent wall-jet were evaluated. It is in this aspect of the research where the shortcomings of the facility became most apparent. There were two problems that prohibited measurement of entire velocity and temperature profiles with forcing: (1) the short-term constant flux nature of the boundary condition

did not hold for the duration needed to measure a full profile and (2) the ac voltage that was supplied to the speaker by the amplifier was accompanied by a small dc component that increased with time. Given the ill-defined nature of the boundary condition and the time required to reach steady state, full profiles with forcing were found to be unrepeatable. It is for this reason that the cases with forcing were restricted to near-wall measurements that could be obtained rapidly and repeatably. Since both the velocity and temperature profiles near the wall were found to be linear, extrapolation from measurements there was used to determine wall shear stress and wall temperature.

The selection of forcing frequencies was determined by the instability characteristics of the flow and the response characteristics of the wall-jet apparatus. Selected frequencies must be in the range of those associated with the instability modes, and they must allow for enough forcing amplitude given the input power limitations. Two frequencies, 48 Hz and 91 Hz, were found to be most appropriate.

For the turbulent wall-jet, the frequencies associated with the viscous instability are higher than those associated with the inviscid instability. In fact, the wall-jet has two rows of vortices. The inner row has a higher frequency than the outer row due to the smaller inner region length scale. According to Katz *et al.*, disturbances in the flow will be most amplified in the outer region when the nondimensional frequency, defined as

$$\beta = (2\pi f \delta_v)/U_m$$

is approximately 0.4, and they will be most amplified in the inner region when $\beta \approx 0.7$. Disturbances to the mean flow introduced at the 48-Hz frequency, for example, are most amplified near the jet exit in the outer region. As the disturbances propagate in X , they become more important with the viscous instability mode. Eventually, the 48-Hz disturbances are no longer amplified in the flow and saturation is observed.

Although the effects of selective forcing on surface shear stress have been shown to be great in historical investigations with even small initial disturbances, a forcing amplitude of 10% was necessary to observe even a small response of the temperature. Waveforms of the hot- and cold-wires are seen to be in phase, but the magnitude of response of the hot-wire is considerably greater than that of the cold-wire as shown in Figure 4.14. This implies that the response of the mean to disturbances is mostly governed by changes in velocity instead of temperature, at least with the velocities and temperatures under investigation.

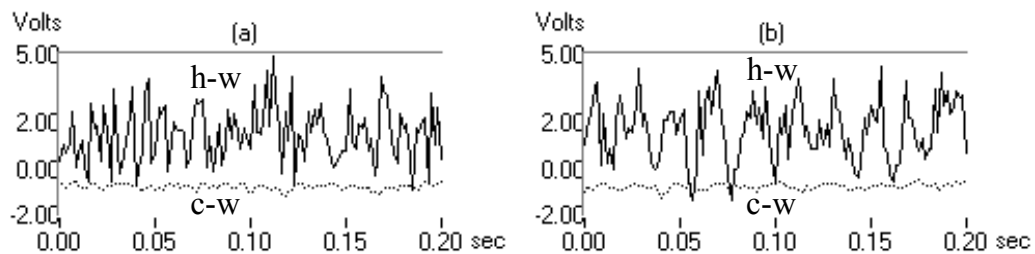


FIGURE 4.14: Unforced (a) and forced (b) waveforms ($X/b = 40$; inner $0.35U_m$).

In the absence of direct surface shear stress and temperature measurements, velocity and temperature measurements in the linear region near the wall were

extrapolated from hot- and cold-wire measurements. Assuming the no-slip condition holds, the local wall shear stress is determined from a single point measurement in the linear region. This enables the determination of the distance from the wall. Assuming the vertical positions of the hot- and cold-wires are identical, the wall temperature is estimated using two points in the linear region. As shown in Figure 4.15, the reduction in shear stress is significantly greater than that of the local temperature scale.

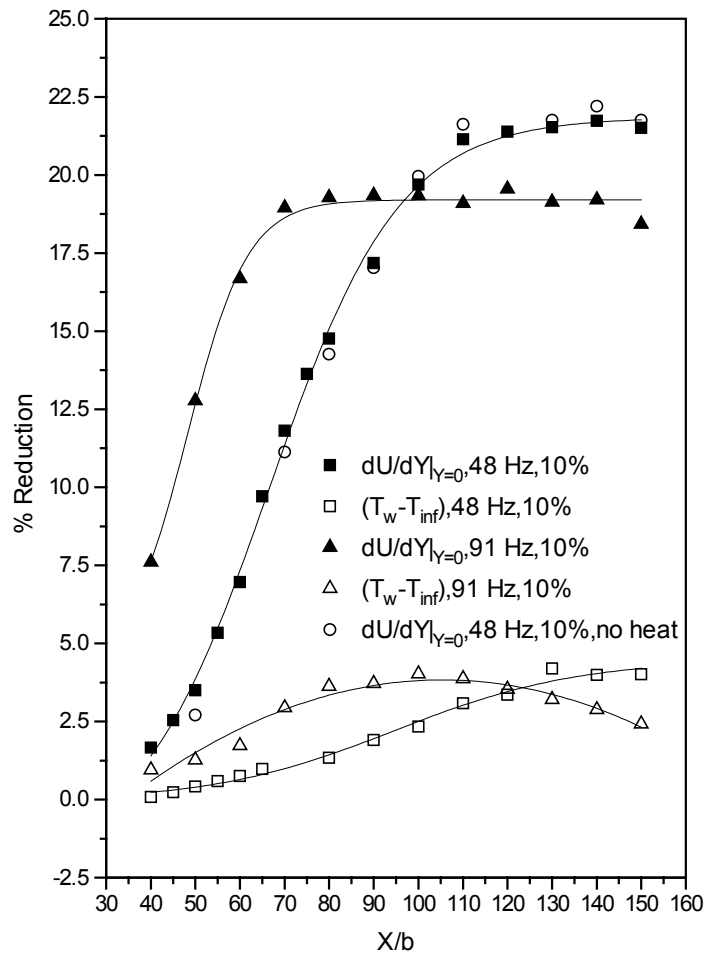


FIGURE 4.15: Effect of forcing on shear stress and wall temperature; 48 Hz and 91 Hz at $\langle u_j' \rangle / U_j \sim 10\%$, with and without a wall heating.

As X/b increases, the effect of forcing on shear stress increases until saturation in both the 48-Hz and 91-Hz cases, an indication of the high level of forcing. Since the amplified range of frequencies in the wall-jet shifts to lower frequencies with increasing streamwise distance, the 91-Hz frequency is the first to saturate. The local wall shear stress in the unforced case is reduced 19% with the introduction of 91-Hz disturbances at

$\langle u_j' \rangle / U_j \sim 10\%$. The lower frequency, however, does not saturate until further downstream and provides increased distance for disturbance amplification, resulting in a maximum shear stress reduction of about 22%. In the 48-Hz case, saturation occurs around $X/b = 120$ compared to $X/b = 80$ in the 91-Hz case. Note that the heated wall showed no influence on the reduction of wall shear stress with forcing, despite an expected destabilization. This is attributed to the high-amplitude forcing causing nonlinear effects and early saturation.

While large reductions in shear stress were observed, only mediocre reductions in the local temperature scale existed in the presence of forcing. Magnitudes of reduction are qualitatively reliable, however, because actual reductions in wall temperature were as much as $0.65\text{ }^\circ\text{C}$, which is much greater than the $\pm 0.1\text{ }^\circ\text{C}$ resolution of the cold-wire. It is believed that selective forcing enhances the vortical structure in the wall-jet. With this enhancement comes an increased exchange of energy between the inner and outer regions of the wall-jet. In the case of the heated wall, cooler air from the inviscid portion of the jet tends to move toward the surface and, likewise, warmer air from the inner region moves outward. Hence, a reduction in wall temperature is observed. Maximum reductions of approximately 4% were measured in both the 48-Hz and 91-Hz cases.

It is slightly apparent from Figure 4.15 and more apparent from Figure 4.16 that the reduction in wall temperature spatially lags the reduction in wall shear stress. Figure 4.16 shows the reductions in shear stress and temperature normalized by the maximum overall reductions. This better illustrates the saturation lag that likely exists.

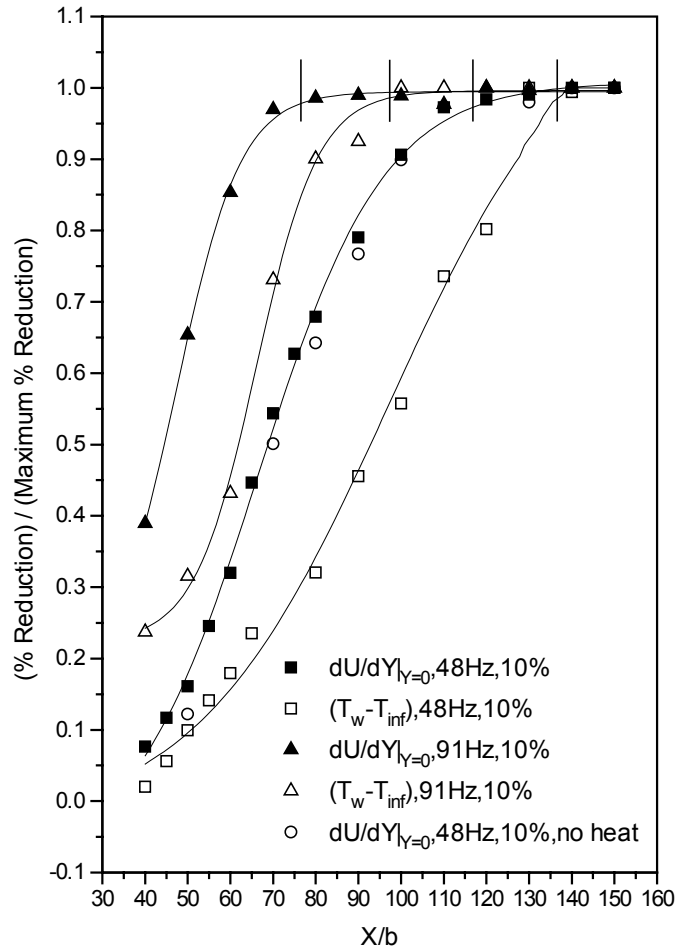


FIGURE 4.16: Effect of forcing on shear stress and wall temperature; 48 Hz and 91 Hz at $\langle u_j' \rangle / U_j \sim 10\%$, with and without a wall heating (normalized by maximum reductions in shear stress and wall temperature).

The spatial lag is probably due to a combination of convection and the difference between the hydrodynamic and thermodynamic inertias. With the introduction of forcing, there is a deceleration of particles near the wall, namely a reduction in shear stress. This deceleration is rapid because the hydrodynamic time constant is small, i.e., the kinematic inertia of the particles is small. Although the reduction in wall shear stress

saturates, the wall temperature continues to decrease downstream because the thermal inertia is relatively large. Convection causes the difference in inertias to be manifested in a spatial saturation lag of around 20 slot heights.

4.3. REPEATABILITY

A serious concern throughout this investigation was repeatability. Given the large temperature changes in the laboratory over the course of a day (± 2 °C), thermal equilibrium was for the most part impossible. This became especially important in light of the temperature compensation procedure used. Since the effect of temperature on the hot-wire voltage was not completely compensated, changes in temperature caused errors in velocity measurement, especially near the wall where sharp gradients in velocity and temperature exist. Data was only repeatable when the temperature of the external flow was allowed to reach a steady state of 22.2 °C and the jet exit temperature reached approximately 23.85 °C. It is needless to say that the attainment of these temperatures, particularly for the amounts of time needed for the heat transfer surface to reach steady state, was difficult. This research became an exercise in room temperature management. The data presented in this thesis is the result of many patient hours. As shown Figure 4.17 through Figure 4.19, the attainable repeatability with consideration of ambient conditions was good in both the unheated reference and heated cases. Wall shear stress was found to be repeatable within 5%, as was the temperature gradient at the wall. U_m , δ_v , and Y_m were within 1.5% while the wall temperature was repeatable within 2%. A repeatability of 5% was attainable with δ_t . The repeatability of the nondimensional

temperature, θ , was not much better than that of T due to the difficulties in reaching steady state.

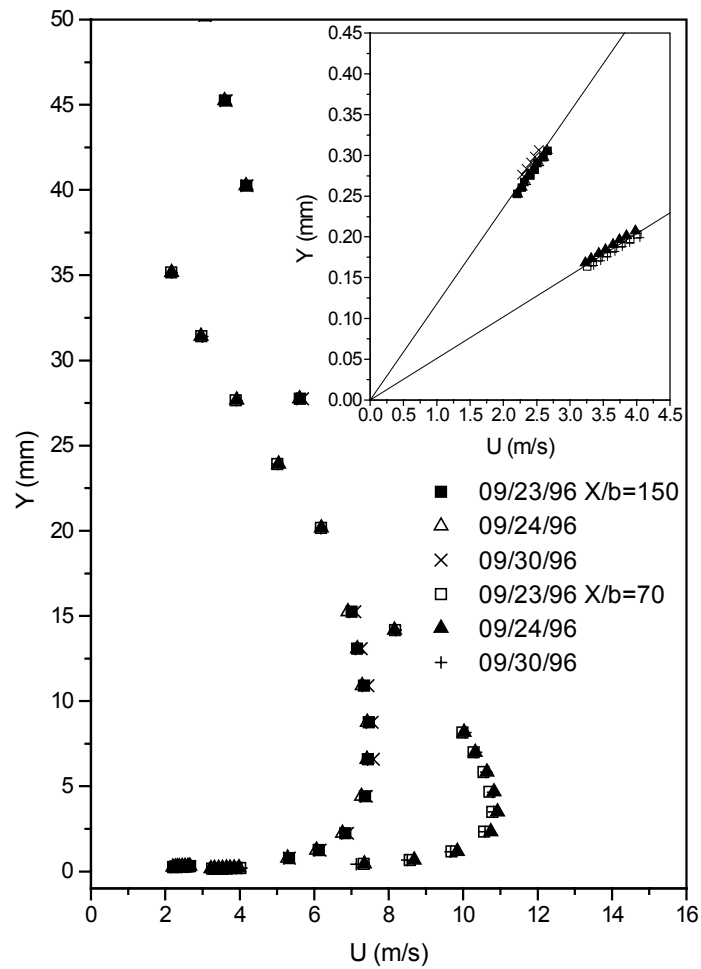


FIGURE 4.17: Repeatability of mean velocity profiles for unheated reference case.

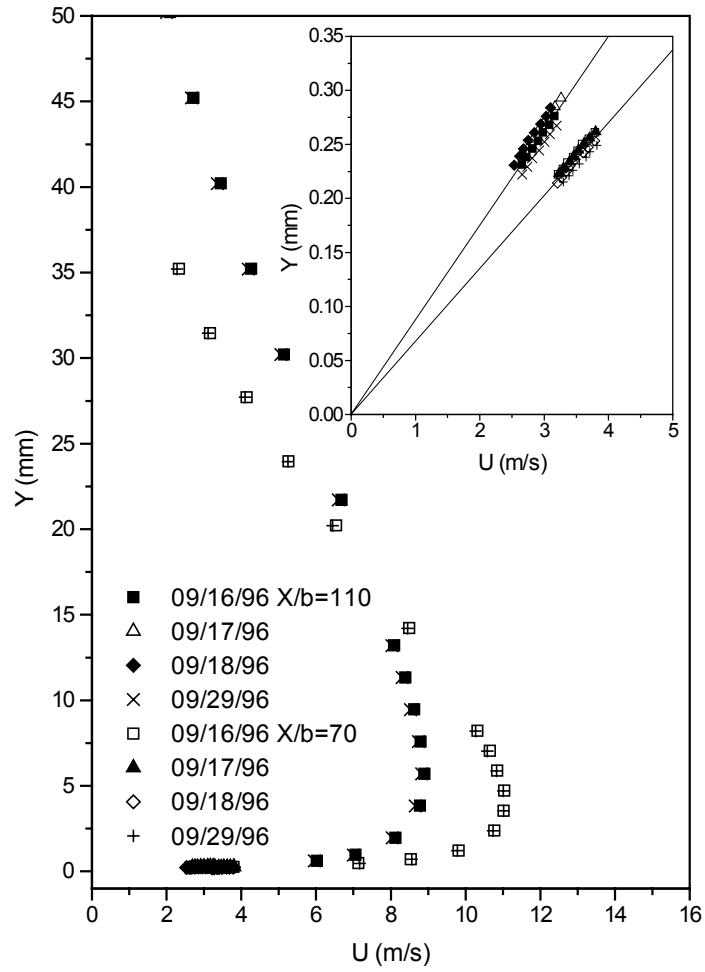


FIGURE 4.18: Repeatability of mean velocity profiles for heated wall case.

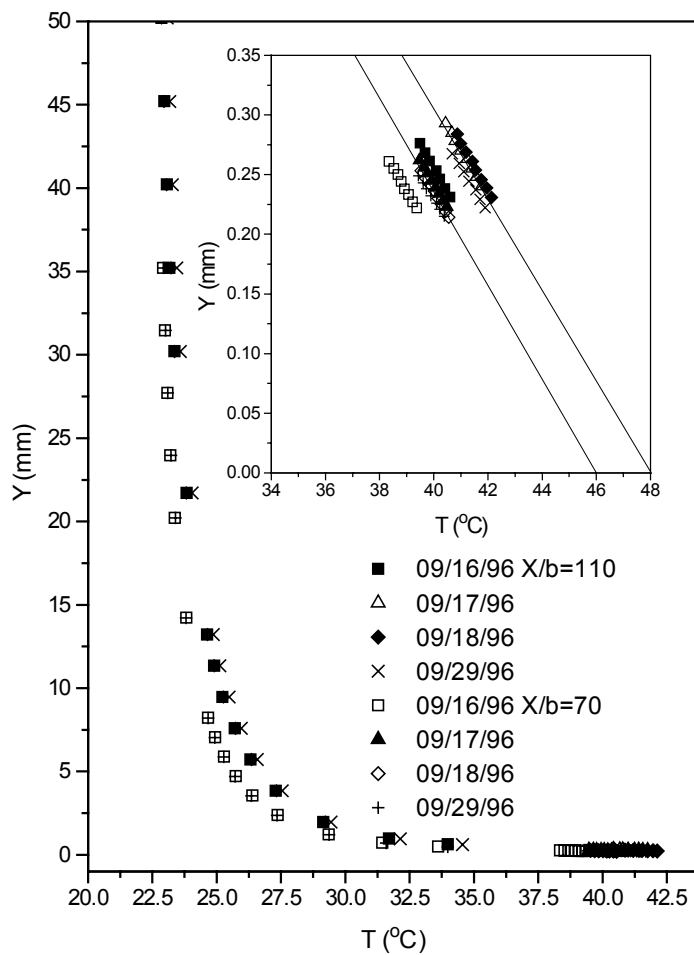


FIGURE 4.19: Repeatability of mean temperature for heated wall case.

5. CONCLUSIONS AND RECOMMENDATIONS

The facility utilized for this investigation is far from ideal due to poor thermal control. Repeatable data was obtained for the turbulent wall-jet, however, which indicates lower wall shear stress and larger fluctuating velocities near a heated surface. Disturbances introduced to the mean flow at 48 and 91 Hz were found to amplify in a streamwise manner in accordance with hydrodynamic stability theory. Reductions in wall shear stress and wall temperature resulted from this selective forcing of the wall-jet instability modes; a maximum reduction in shear stress of 22% was observed with a simultaneous reduction in the local temperature scale of approximately 4%, indicating that selective forcing is a viable technique for reducing drag and increasing heat transfer to the wall. Wall temperature reduction apparently spatially lags wall shear stress reduction as well. If $Pr_t = \epsilon_H / \epsilon_M$ for the unforced case, as claimed by the Reynolds analogy, then the results reported herein indicate that the introduction of oscillations alters Pr_t near the wall. Further study of the turbulent wall-jet with heat transfer is suggested to gain a better understanding of the effects of selective forcing.

Future work on the turbulent wall-jet with heat transfer should be precursored by an improvement of the hot-wire temperature compensation procedure, fabrication of a well-defined constant flux surface, improvement of ambient thermal control, attainment of a micro triple-wire probe suitable for near-wall measurements, and installation of direct surface temperature and shear stress measurement devices. Using a look-up table to determine the change in hot-wire voltage with temperature for a specific velocity

should improve the repeatability of the velocity measurement, while using a well-defined constant flux surface will enable more reliable and quantifiable results. Thermal control of the environment should be improved to the order of ± 0.1 °C in order to make ambient fluctuations small compared to the temperature differences under investigation. A temperature-compensated micro x-wire is recommended for future investigations so that velocity-temperature correlations can be obtained and the consistency of the data can be checked, and direct measurement of surface temperature and wall shear stress with micro-electro-mechanical sensors would greatly simplify the procedure of evaluating the effects of forcing.

REFERENCES

- [1] Launder, B.E. and Rodi, W., "The Turbulent Wall Jet", *Prog. Aerospace Sci.*, v. 19, p. 81, 1981.
- [2] Launder, B.E. and Rodi, W., "The Turbulent Wall Jet- Measurements and Modeling", *Ann. Review Fluid Mech.*, p. 429, 1983.
- [3] Zhou, M.D., Rothstein, J., and Wygnanski, I., *Proceedings 11th Australian Fluid Mechanics Conference*, p. 407, 1992.
- [4] Katz, Y., Hover, E., and Wygnanski, I., "The Forced Turbulent Wall Jet", *J. Fluid Mech.*, v. 242, p. 577, 1992.
- [5] Lebedev, V.P., Lemanov, V.V., Misyura, S. YA., and Terekhov, V.I., "Effects of Flow Turbulence on Film Cooling Efficiency", *Int. J. Heat and Mass Trans.*, v. 38, n.11, p. 2117, 1995.
- [6] Moffat, R. and Maciejewski, P.K., "Heat Transfer with Very High Free-Stream Turbulence", NASA Grant NAG3-522, Proceedings of the 1985 Turbine Engine Hot Section Technology Conference (NASA Conference publication 2405), p. 203.
- [7] MacMullin, R., Elrod, W., and Rivir, R., "Free-Stream Turbulence from a Circular Wall Jet on Flat Plate Heat Transfer and Boundary Layer Flow", *ASME Journal of Turbomachinery*, v. 111, p. 78, 1989.
- [8] Goldstein, R.J., "Film Cooling", *Advances in Heat Transfer*, J.P. Hartnett and T.F. Irvine, Jr. eds., v. 7, p. 321, Academic Press, New York, 1972.
- [9] Dec, J.E. and Keller, J.O., "Time Resolved Gas Temperatures in the Oscillating Turbulent flow of a Pulse Combustor Tail Pipe", *Combustion and Flame*, v. 80, p.358, 1990.
- [10] Arpaci, V.S., Dec., J.E., and Keller, J.O., "Heat Transfer in Pulse Combustor Tail Pipes", *Combustion Science and Technology*, 1992.
- [11] Quintana, D., Amitay, M., Seidel, J., Fasel, H., Ortega, A., and Wygnanski, I.,

“Film Cooling by a Pulsating Wall Jet”, AFOSR Grant F49620-94-1-0131
Progress Report, 1995.

- [12] Kays, W.M. and Crawford, M.E., *Convective Heat and Mass Transfer*, McGraw-Hill, New York, 1993.
- [13] Wygnanski, I., Katz, Y., and Hover, E., “On the Applicability of Various Scaling Laws to the Turbulent Wall Jet”, *J. Fluid Mech.*, v. 234, p. 669, 1992.
- [14] Glauert, M.B., “The Wall Jet”, *J. Fluid Mech.*, v. 1, p. 625, 1956.